Molecular Cell, Vol. 20, 771–781, December 9, 2005, Copyright ©2005 by Elsevier Inc. DOI 10.1016/j.molcel.2005.10.014

# Detection of High-Affinity and Sliding Clamp Modes for MSH2-MSH6 by Single-Molecule Unzipping Force Analysis

Jingjing Jiang,[1,3] Lu Bai,[2,3] Jennifer A. Surtees,[1] Zekeriyya Gemici,[1] Michelle D. Wang,[2] and Eric Alani[1,*]
[1] Department of Molecular Biology and Genetics
[2] Department of Physics
Cornell University
Ithaca, New York 14853

## Summary

**Mismatch repair (MMR) is initiated by MutS family proteins (MSH) that recognize DNA mismatches and recruit downstream repair factors. We used a single-molecule DNA-unzipping assay to probe interactions between *S. cerevisiae* MSH2-MSH6 and a variety of DNA mismatch substrates. This work revealed a high-specificity binding state of MSH proteins for mismatch DNA that was not observed in bulk assays and allowed us to measure the affinity of MSH2-MSH6 for mismatch DNA as well as its footprint on DNA surrounding the mismatch site. Unzipping analysis with mismatch substrates containing an end blocked by *lac* repressor allowed us to identify MSH proteins present on DNA between the mismatch and the block, presumably in an ATP-dependent sliding clamp mode. These studies provide a high-resolution approach to study MSH interactions with DNA mismatches and supply evidence to support and refute different models proposed for initiation steps in MMR.**

## Introduction

Mismatch repair (MMR) plays an important role in maintaining genome stability by correcting DNA biosynthetic errors and by participating in the cellular response to some types of DNA damage. This system improves the fidelity of DNA replication by about 1000-fold by excising DNA mismatches in the newly replicated strand, which arise as the result of polymerase misincorporation errors. Defects in MMR significantly increase the mutation rate and have been implicated in hereditary forms of colon cancer (Schofield and Hsieh, 2003; Heinen et al., 2002).

In prokaryotes and eukaryotes, the MSH family of MMR proteins specifically bind to DNA mismatches in vitro. In eukaryotes, the MSH2-MSH6 complex recognizes single base pair mismatches and small insertion/deletion loop mismatches, while the MSH2-MSH3 complex recognizes insertion/deletion loops up to 12 nt in size. The MLH MMR proteins, primarily MLH1-PMS1 in *S. cerevisiae*, are thought to act as matchmaker proteins. They interact in an ATP-dependent fashion with MSH proteins bound to mismatch DNA and appear to be required to activate downstream repair factors. These downstream events, which result in the excision and resynthesis of the newly synthesized DNA strand, also appear to be coordinated with the DNA replication machinery (reviewed in Kunkel and Erie [2005]).

It is difficult to reconcile the high specificity of MMR in vivo with that seen in gel shift assays in which MSH complexes typically display a 10- to 30-fold specificity for mismatch compared to homoduplex DNA (Kijas et al., 2003; Marsischky and Kolodner, 1999; Mendillo et al., 2005; Yang et al., 2005). One explanation is that MMR specificity is accomplished by combinatorial interactions involving multiple components, each of which displays modest selectivity (Bowers et al., 2000). Alternatively, MSH proteins have distinct and highly specific modes of DNA binding that are difficult to observe by current methods. For example, gel shift assays involving linear substrates are thought to underestimate mismatch binding specificity because the MSH proteins display a DNA end binding activity (Wang et al., 2003; Mendillo et al., 2005; Yang et al., 2005).

In addition to mismatch binding, the MSH proteins display ATP binding and hydrolysis activities that are activated in the presence of mismatch DNA substrates. These activities are important for modulating mismatch recognition and for the recruitment of additional MMR factors (reviewed in Schofield and Hsieh [2003], Kunkel and Erie [2005]). In these studies, ATP and its nonhydrolyzable analog ATP$\gamma$S dramatically decreased the affinity of the bacterial, yeast, and human MutS homologs for mismatch DNA. Three models have been developed to explain the loss of mismatch binding specificity in the presence of ATP. The first two models (Blackwell et al., 1998; Gradia et al., 1997) proposed that, in the presence of ATP, the MSH proteins move away from the mismatch site in search of downstream repair factors. One model (Allen et al., 1997; Blackwell et al., 1998) proposed that MSH movement is powered by ATP hydrolysis, with the end result being the extrusion of the mismatch site into a loop structure. In contrast, Gradia et al. (1997) proposed a molecular switch model in which mismatch binding triggers an ADP → ATP exchange that enables the MSH proteins to enter a sliding clamp diffusion mode leading to the loading of multiple MSH complexes at a single mismatch site. This loading is thought to act as a landmark for excision enzymes to remove DNA from a strand-discrimination entry site to the mismatch. In a third model (Junop et al., 2001), the MutS ATPase activity acts in a proofreading role to verify mismatch recognition and authorize repair. In this model, the MSH proteins remain bound to the mismatch site while activating downstream repair functions.

We used a single-molecule approach to ask whether the MSH proteins display a higher mismatch binding specificity than was measured by bulk DNA binding assays and to determine the role that ATP plays in modulating this specificity. This analysis has several advantages over traditional bulk studies. First, unlike bulk binding assays in which the experimental data are averaged over large number of molecules, a single-molecule approach allows one to examine individual MSH-DNA complexes so that heterogenous populations can be differentiated. Second, DNA substrates used in single-molecule studies

*Correspondence: eea3@cornell.edu
[3] These authors contributed equally to this work.

can often be much longer (e.g., several kilobases) than those used in bulk studies, in which substrates are typically less than 100 bp. Thus, substrates approaching those recognized by MMR proteins in vivo can be examined. Third, single-molecule assays can ultimately be used to track the activity of MSH2-MSH6 in real time with a high temporal resolution so that the rapid kinetic behavior of individual molecules can be detected. To probe the binding of MSH proteins to mismatch DNA, we used a method called unzipping force analysis (Koch et al., 2002) to measure MSH2-MSH6 on single molecules of mismatch DNA. As described below, this high-resolution method allowed us to detect high-affinity mismatch binding and sliding clamp modes for MSH2-MSH6.

## Results

Single-molecule unzipping analysis measures the effect of protein association and sequence context on the force required to unwind duplex DNA (Koch et al., 2002). In this study, 1.1 kb duplex DNA molecules containing single DNA mismatches were unwound in the presence or absence of the MSH2-MSH6 mismatch binding complex (Figures 1 and 2). Unwinding was accomplished by anchoring one end of a duplex DNA to a microscope coverslip binding chamber through a digoxigenin/antidigoxigenin linkage. This substrate contains a biotinylated base adjacent to a nick located in the middle of the duplex DNA. In the unzipping assay, this base is attached to a streptavidin-coated microsphere held in a feedback-enhanced optical trap. DNA becomes unzipped as the coverslip is moved away from the optical trap; simultaneously recording the coverslip position and the unzipping force yields a force curve (Figure 3). This method can detect the presence of a protein bound to a specific site on a DNA substrate due to the transient obstruction of the unzipping fork at the protein-DNA interface. The obstruction results in an increase in the unzipping force required to unwind DNA followed by a sudden drop in the force once the protein-DNA complex has been disrupted. As described in the Experimental Procedures, we constructed unzipping substrates that contained G/T, +1 (G insertion), and +8 (GTGTGTGT) mismatches located 356–383 bp from a biotin label that serves as the initiation point for unzipping.

The unzipping force curves for the G/T, +1, and +8 substrates were compared to those obtained for the homoduplex G/C substrate (Figure 2). Because the unzipping force is determined by DNA base pairing energies (Bockelmann et al., 1997, 1998; Essevaz-Roulet et al., 1997), mismatches encountered during DNA unzipping should result in a localized drop in the unzipping force. Consistent with this prediction, the mismatch substrates showed reduced unzipping force in the region surrounding the mismatch compared to the homoduplex G/C substrate (Figure 2). The drop in unzipping force caused by the +8 loop was present in all 28 traces (Figure 2A). For the G/T and +1 mismatches, the drop in unzipping force was relatively small but statistically significant ($p < 0.005$, Student's t test) and is reflected by the average unzipping curve (Figures 2B and 2C). These data suggest that our unzipping templates contain the mismatch at the designed location and are homogeneous (Experimental Procedures).

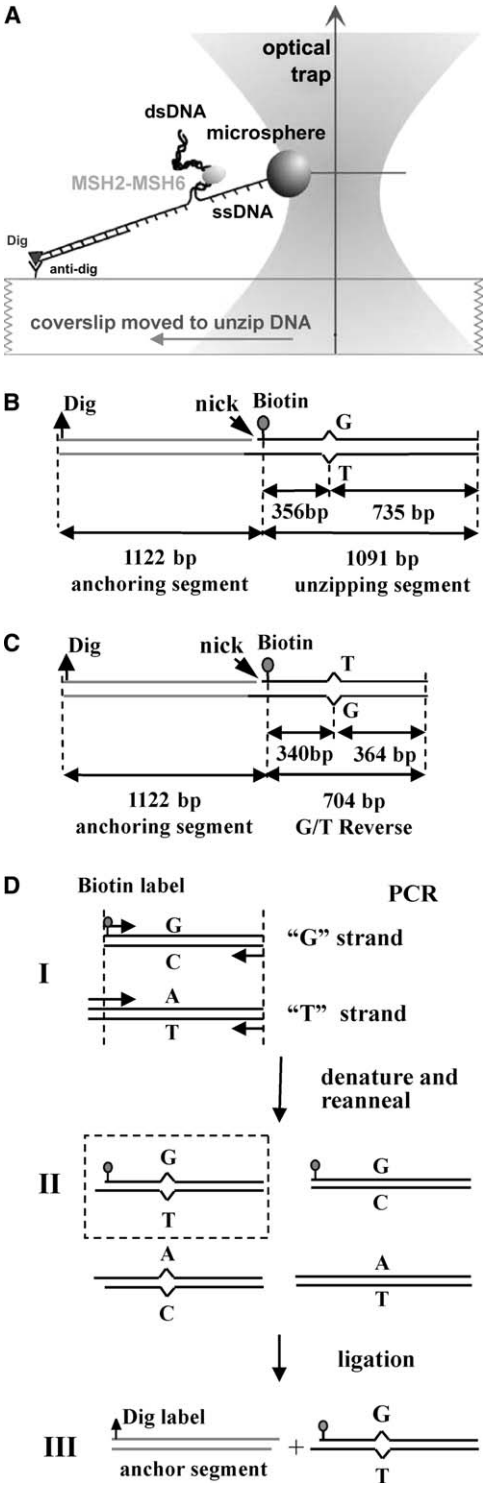


Figure 1. DNA Substrates Used in Unzipping Assay

(A) Cartoon outlining the experimental configuration of the single-molecule DNA unzipping assay. See text for details.

(B and C) Diagrams of the G/T (B) and G/T reverse (G/T-R, [C]) mismatch substrates.

(D) Construction of the G/T mismatch substrate. Two PCR products, G/C and A/T, (I) were denatured, reannealed, and then treated with alkaline phosphatase as described in the Experimental Procedures. Among the four reannealing products (II), only the G/T segment could be ligated to the anchoring segment to form the nicked G/T mismatch substrate (III).

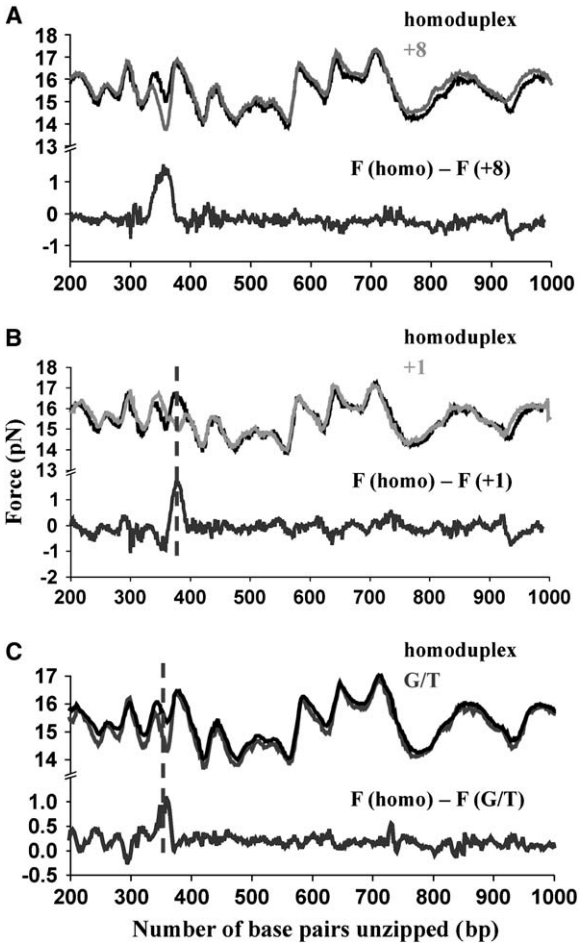


Figure 2. Comparison of the Force Required to Unzip Homoduplex and Heteroduplex DNA Substrates

(A) Average unzipping force curve obtained for the homoduplex G/C (n = 25, black curve) and +8 (n = 28, gray curve) substrates.
(B and C) Data presented as in (A), except with the +1 mismatch (n = 20, gray curve in [B]) and G/T mismatch (n = 30, dark gray curve in [C]) substrates.

### MSH2-MSH6 Binds to G/T and +1 Mismatches with High Specificity

To probe the binding of MSH2-MSH6 to the DNA templates, MSH2-MSH6 was incubated with mismatch DNA for 10 min at 24°C before individual molecules were subjected to unzipping. Previous studies suggested that this incubation time was sufficient to reach equilibrium for MSH2-MSH6 binding (Kijas et al., 2003). Figure 3 shows individual force curves for the G/T DNA substrate incubated in the absence (Figure 3A) or presence (Figure 3B) of 8 nM MSH2-MSH6 after alignment (Experimental Procedures). The presence of MSH2-MSH6 resulted in an increase in the unzipping force peaks that clustered near the site of the G/T mismatch; this was not seen with the DNA substrate alone. Therefore, this elevated force cluster likely corresponds to the disruption of the MSH2-MSH6-mismatch complex. Similar data were obtained in the individual traces for MSH2-MSH6 binding studies performed with the +1 substrate (data not shown).

The specificity of MSH2-MSH6 for the mismatch site is shown in the average of all the individual force traces (Figures 3C–3E). For experiments performed with the G/T and +1 substrates in the presence or absence of MSH2-MSH6, the only significant difference in the average unzipping force was in the vicinity of the mismatch (Figures 3C and 3E), suggesting that this represents the primary binding site for MSH2-MSH6 on the DNA template. The binding affinity of MSH2-MSH6 to the G/T and +1 mismatch sites was determined by analyzing individual unzipping force curves (Figure 4). By focusing on a narrow window surrounding an elevated force cluster (Figure 4A), MSH2-MSH6 binding events were identified when the elevated force exceeded a defined threshold (Figure 4B; Experimental Procedures). Of the 103 G/T substrate traces performed in the presence of 8 nM MSH2-MSH6, 60 were identified that displayed MSH2-MSH6 binding. The ratio between the unbound and bound mismatch sites reflects the dissociation constant, $K_d$, of the MSH2-MSH6-mismatch complex where $K_d$ = [free MSH2-MSH6] [free G/T]/[MSH2-MSH6 − G/T]. The $K_d$ for the G/T mismatch, 5.7 nM, was within the range obtained in bulk studies (0.2–41 nM; Gradia et al. [1997], Marsischky and Kolodner [1999], Hess et al. [2002]). As shown in Table 1, MSH2-MSH6 displayed similar binding affinity for the +1 mismatch.

Elevated force events were occasionally observed in addition to those at the mismatch site, and their location displayed a random distribution (Figure 3B). For 103 traces performed with the G/T substrate, 14 such events were observed, corresponding to an average frequency of $\sim 2.7 \times 10^{-4}$ per base pair. We hypothesize that these events reflect nonspecific binding of MSH2-MSH6 to homoduplex DNA as well as adhesion of the DNA templates to the sample chamber. The latter is more likely because elevated force events were observed with a similar frequency ($\sim 2.1 \times 10^{-4}$/bp) in the absence of MSH2-MSH6 (Figure 3A). Therefore, the high force events caused by nonspecific binding of MSH2-MSH6 to homoduplex DNA are likely to occur with an even lower frequency, at least three orders of magnitude lower than seen at a mismatch site (~0.5 per base pair). These data indicate that the selectivity of binding for MSH2-MSH6 for mismatch DNA in this system is much higher than reported in bulk assays involving binding of MSH2-MSH6 to short (<80 bp) oligonucleotides (10- to 30-fold, Kijas et al. [2003], Marsischky and Kolodner [1999]). Consistent with this, elevated force events were rarely observed with the homoduplex G/C substrate incubated in the presence of 8 or 20 nM MSH2-MSH6 ($\sim 2.0 \times 10^{-4}$ per base pair frequency, Figure 3D).

To test whether MSH2-MSH6-homoduplex binding events were not observed because they displayed an undetectable elevation in unwinding force, unzipping experiments were performed in the presence of competitor DNA. Uncut 6.8 kB plasmid DNA (pEAM128) (6 nM) was preincubated with 8 nM MSH2-MSH6 and then added to reaction chambers containing 0.1 pM immobilized G/T substrate. The presence of homoduplex competitor DNA lowered the occupancy ratio of MSH2-MSH6 at the G/T mismatch site from 50% to 30% (13 mismatch binding events in 44 traces). The decrease in binding to the G/T mismatch site indicates that 4.6 nM MSH2-MSH6 was sequestered by ~41 μM of homoduplex base pairs

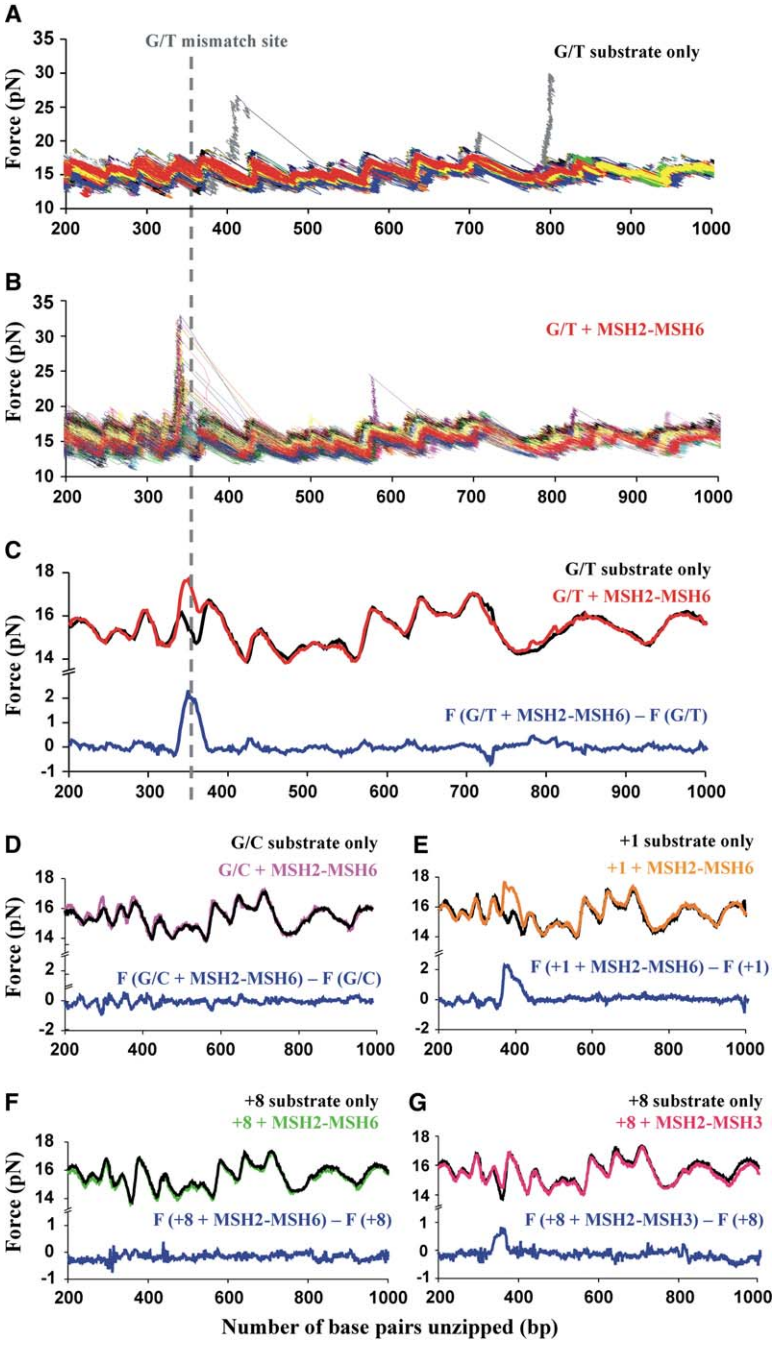


Figure 3. MSH2-MSH6 Specifically Binds to Mismatch Sites

(A and B) Individual force traces for the G/T substrate in the absence ([A], n = 30) or presence ([B], n = 103) of 8 nM MSH2-MSH6. The traces in (B) indicate that MSH2-MSH6 binding resulted in a clustering of elevated force peaks near the G/T mismatch site (dashed line).

(C) Average force curves for the traces shown in (A) (G/T substrate, black curve) and (B) (G/T substrate incubated with 8 nM MSH2-MSH6, red curve). The blue curve represents the difference between the two averaged unzipping forces.

(D–G) Similar data sets as shown in (C), except the DNA substrate is homoduplex G/C for (D) (n = 25 without MSH2-MSH6, n = 30 with 8 nM MSH2-MSH6), +1 for (E) (n = 20 without MSH2-MSH6, n = 80 with 8 nM MSH2-MSH6), and +8 for (F) and (G). (F) shows the average traces without MSH2-MSH6 (n = 24) and with 8 nM MSH2-MSH6 (n = 16), and (G) shows the average traces without MSH2-MSH3 (n = 24) and with 8 nM MSH2-MSH3 (n = 22). In each panel, the curves show the average unzipping force for the mismatch substrate subtracted from that obtained in the presence of the indicated MSH complex.

($K_d$/[free MSH2-MSH6] = [free G/T]/[MSH2-MSH6 – G/T] = occupancy ratio). Thus, the binding frequency of MSH2-MSH6 on homoduplex sites in this experiment is $\sim 1 \times 10^{-4}$ per base pair, which supports the conclusion that, under the MSH and DNA concentrations used in this study, the binding affinity of MSH2-MSH6 for homoduplex DNA is at least three orders of magnitude lower than for a mismatch site.

The unzipping assay was also used to test the binding of MSH2-MSH3 on the +8 substrate. As shown in Figure 3G, incubation with 8 nM MSH2-MSH3 resulted in an elevated unzipping force in the vicinity of the +8 loop mismatch, indicating specific MSH2-MSH3 binding to that site (p = 0.005). In contrast, specific binding was not observed when MSH2-MSH6 was tested with the +8 loop (Figure 3F). This result is consistent with in vivo studies showing that MSH2-MSH6 is not involved in repairing +8 loop mismatches (Sia et al., 1997), and in vitro footprinting showing that MSH2-MSH3 but not MSH2-MSH6 conferred specific protection of a +8 duplex oligonucleotide (data not shown).

### Mapping of the Force Elevation Peaks to the Base Pair Level Indicates that MSH2-MSH6 Binds Asymmetrically to Mismatch DNA

The elevated force peak location is thought to mark the boundary of the MSH2-MSH6-DNA interface on one side of the mismatch. As shown for the G/T substrate

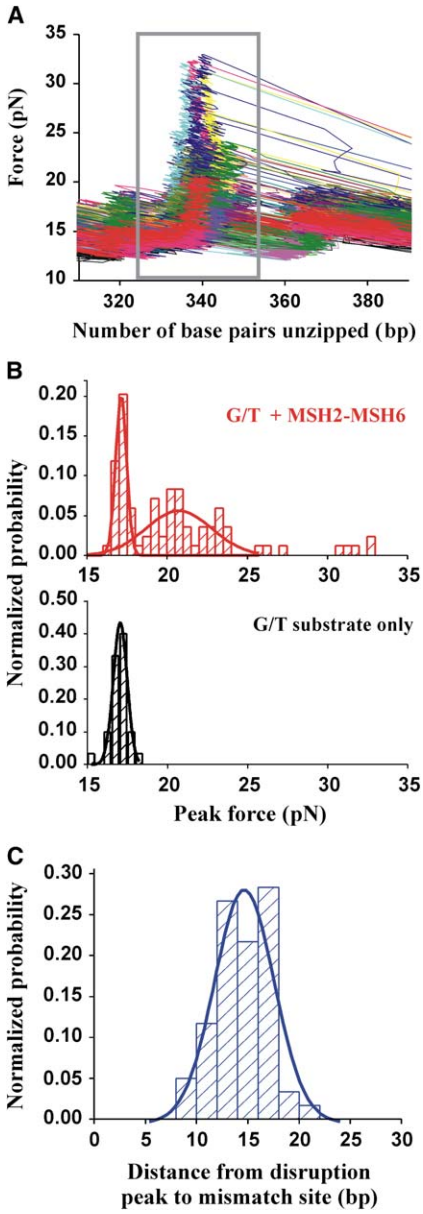


Figure 4. Position of the MSH2-MSH6-Dependent Elevated Force Peaks Relative to the Mismatch Site

(A) Individual force curves for the G/T template in the presence of 8 nM MSH-MSH6. The data are shown for a 30 bp window containing the peak cluster.

(B) Histogram of the peak force value of each individual trace within the 30 bp window in the presence (top panel) or absence (bottom panel) of 8 nM MSH2-MSH6. In the presence of MSH2-MSH6, the histogram displayed a bimodal distribution that was fit to a double Gaussian function. The Gaussian centered at the lower force levels aligns well with that of DNA incubated in the absence of MSH2-MSH6. By setting the intersection point of the two Gaussian functions as a threshold, traces with a higher peak force were designated as those showing MSH2-MSH6 binding.

(C) Histogram showing the distance from the elevated force peak observed in the presence of MSH2-MSH6 to the G/T mismatch site. Data were fit to a single Gaussian distribution.

(Figure 4C), the peak position distribution fits into a single Gaussian distribution that is centered 14 bp upstream of the G/T mismatch site (Figure 4C; Experimental Procedures). The standard deviation of the Gaussian,

Table 1. Binding Affinity of MSH2-MSH6 to Mismatch Substrates

| Substrate | ATP (μM) | Number of Traces | % Bound (± SD) | $K_d$ (nM) |
|---|---|---|---|---|
| G/T | – | 103 | 58 ± 5 | 5.7 ± 1.2 |
| G/T | 20 | 28 | 11 ± 6 | – |
| G/T | 100 | 32 | 3 ± 3 | – |
| G/T-R | – | 57 | 56 ± 6 | 6.3 ± 1.7 |
| +1 | – | 80 | 45 ± 6 | 9.8 ± 2.4 |
| +1 | 20 | 20 | 20 ± 9 | – |
| +1 | 100 | 18 | 0 | – |
| +1-R | – | 59 | 54 ± 6 | 6.8 ± 1.9 |

In all experiments, MSH2-MSH6 was present at 8 nM.

2–3 bp, reflects the typical accuracy of our mapping technique, suggesting that the elevated force events occurred at a unique, apparently fixed, position. To determine whether MSH2-MSH6 binds the G/T mismatch in a directional manner, we mapped the elevated force peak locations on both sides of mismatch by unzipping mismatch substrates in both orientations relative to the anchoring segment (forward [F] and reverse [R]; Figure 2; Experimental Procedures). These experiments were performed on G/T and +1 mismatch substrates (Figure 5).

The G/T-R and +1-R substrates displayed similar binding affinities compared to their forward counterparts (Table 1). Like the forward substrates, the location of elevated force events relative to the mismatch site followed a single Gaussian distribution (Figures 5C and 5D). However, the peaks were not symmetric with respect to the mismatch site. For the G/T mismatch, the mean distance (± standard error) between the elevated force peak and mismatch was 14.3 ± 0.3 (n = 103) and 6.2 ± 0.3 (n = 57) bp for the forward and reverse unzipping experiments, respectively. For the +1 mismatch, these values were 11.5 ± 0.3 (n = 80) and 8.7 ± 0.3 (n = 59) bp, respectively. Interestingly, the total region "protected" by MSH2-MSH6, ~20 bp, was similar for the G/T and +1 substrates and was consistent with bulk footprinting data obtained for yeast and human MSH2-MSH6 bound to mismatch DNA (Gradia et al., 1997; Kijas et al., 2003).

Using the forward and reverse mismatch substrates, we also determined the magnitude of the elevated peak force. Because the unzipping force of DNA is sequence dependent, we corrected the elevated force events observed in the forward and reverse unzipping experiments by subtracting the force observed with DNA in the absence of MSH2-MSH6 (Experimental Procedures). The histograms presented in Figures 5E and 5F show different force values for the forward and reverse unzipping experiments involving the G/T, G/T-R, +1, and +1-R substrates. Theoretical work has shown that the peak force value is directly related to the activation barrier of disrupting a protein-DNA complex but not necessarily the protein binding affinity (Evans, 2001). Therefore, the different force magnitudes that were observed on the different sides of the mismatch are likely to indicate an asymmetry in the interactions between MSH2-MSH6 and sequences surrounding the mismatch site. This information, together with the footprint data, suggests that there is a preferred orientation for MSH2-MSH6 binding to the G/T and +1 mismatch sites.

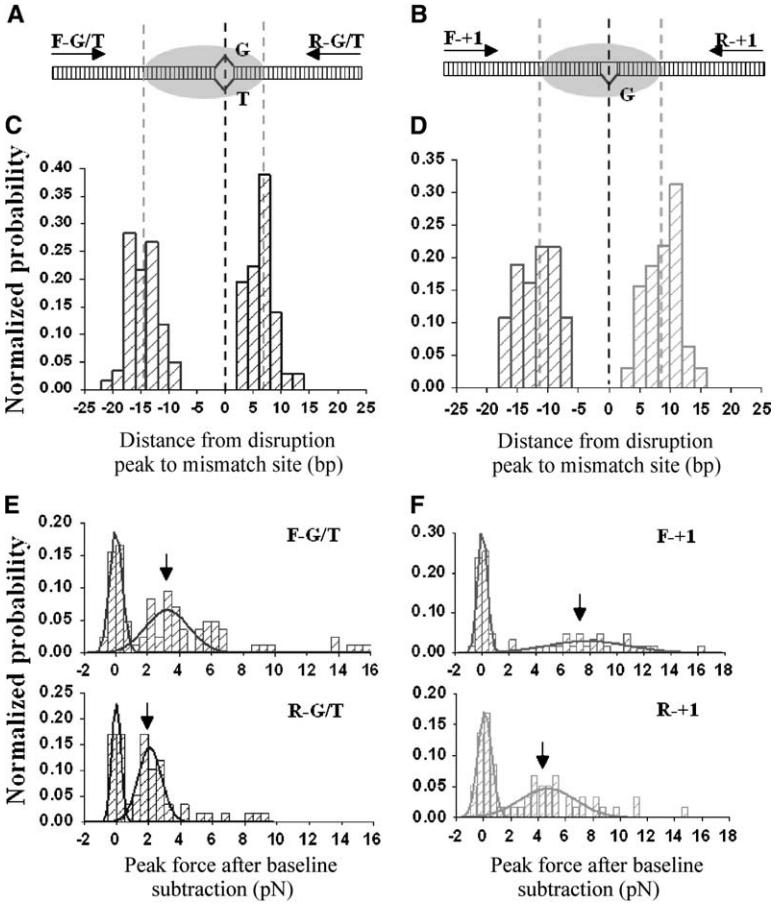


Figure 5. MSH2-MSH6 Displays Asymmetric Binding at Mismatch Sites

(A and B) Cartoon of MSH2-MSH6 binding to the G/T (A) and +1 (B) mismatch substrates. Arrows indicate the direction of unzipping for the forward (F) and reverse (R) substrates.

(C and D) Histograms indicating the distance from the MSH2-MSH6 disruption peaks to the G/T (C) or +1 (D) mismatch sites. The average distance (± SEM) to the G/T mismatch was 14.3 ± 0.3 and 6.2 ± 0.3 bp for the G/T and G/T-R substrates, respectively. For the +1 mismatch, the values were 11.5 ± 0.3 and 8.7 ± 0.3 bp for +1 and +1-R, respectively.

(E and F) Normalized histograms showing the peak force values (arrows) observed in each trace in a 30 bp window surrounding the G/T (E) and +1 (F) mismatch substrates. Histograms were fit to double Gaussian distributions.

### ATP Lowers the Binding Affinity of MSH2-MSH6 to Mismatch Substrates

Previous dissociation studies have shown that mismatch-specific binding by the MSH proteins is rapidly lost in the presence of ATP (reviewed in Kunkel and Erie [2005]). Consistent with this, we found in the unzipping assay that the addition of 20–100 μM ATP to G/T and +1 substrates preincubated for 5 min with MSH2-MSH6 resulted in the loss of mismatch-specific binding events (Table 1). For the prebound G/T substrate incubated with 100 μM ATP, only one binding event was observed (n = 32); for the +1 substrate, no binding events were observed (n = 18). The low probability of binding at the mismatch site in the presence of ATP made it difficult to accurately measure the binding affinity. Based on this limited sample number, we estimate that the $K_d$ for binding of MSH2-MSH6 to the G/T substrate in the presence of 100 μM ATP was at least 10-fold higher than in the absence of ATP. This increase is consistent with $K_d$ values obtained in previous bulk studies (Gradia et al., 1997; Blackwell et al., 1998; Iaccarino et al., 1998; Marsischky and Kolodner, 1999; Joshi et al., 2000). We observed a similar increase in $K_d$ in the presence of 100 μM ATPγS (data not shown).

The binding affinity parameter $K_d$ represents the ratio of on-to-off binding rates. To better understand the effect of ATP on mismatch binding, we measured the dissociation (off) rate of MSH2-MSH6 from the G/T substrate ($t_{1/2}$ = 12 min, see Figure S1 in the Supplemental Data available with this article online). This value was similar to that seen in previous bulk studies with MutS (~10 min, Schofield et al. [2001]). In the presence of ATP, loss of the elevated force peaks was too rapid to determine the dissociation rate by the unzipping method (data not shown) and is consistent with studies suggesting that the ATP-dependent dissociation rate for MutS to mismatch DNA is on the order of seconds (Schofield et al., 2001).

### Unzipping Analysis with Mismatch Substrates Containing an End Blocked by *lac* Repressor Supports an ATP-Dependent Sliding Clamp Mode for MSH2-MSH6

As described in the Introduction, three models have been proposed to explain the role of ATP and ATP hydrolysis in initiation steps of MMR. Major differences between the models include the following: (1) whether ATP-induced release of MSH2-MSH6 from the mismatch substrates occurs by direct dissociation, sliding, or both; and (2) whether this release depends on ATP hydrolysis. To explore these models, we carried out unzipping measurements using DNA substrates end blocked by the biotin-attached microsphere and *lac* repressor (LacI) bound to a *lac*O1 site located 122 bp downstream from the G/T mismatch (Figure 6A, Experimental Procedures). LacI binds to the *lac*O1 site with an extremely high affinity (pM–nM, depending on buffer conditions) and a slow dissociation rate (~20 min half-life; King et al. [2003]). In addition, Mendillo et al. (2005) showed that LacI can act as reversible block for dissociation of MSH2-MSH6 though

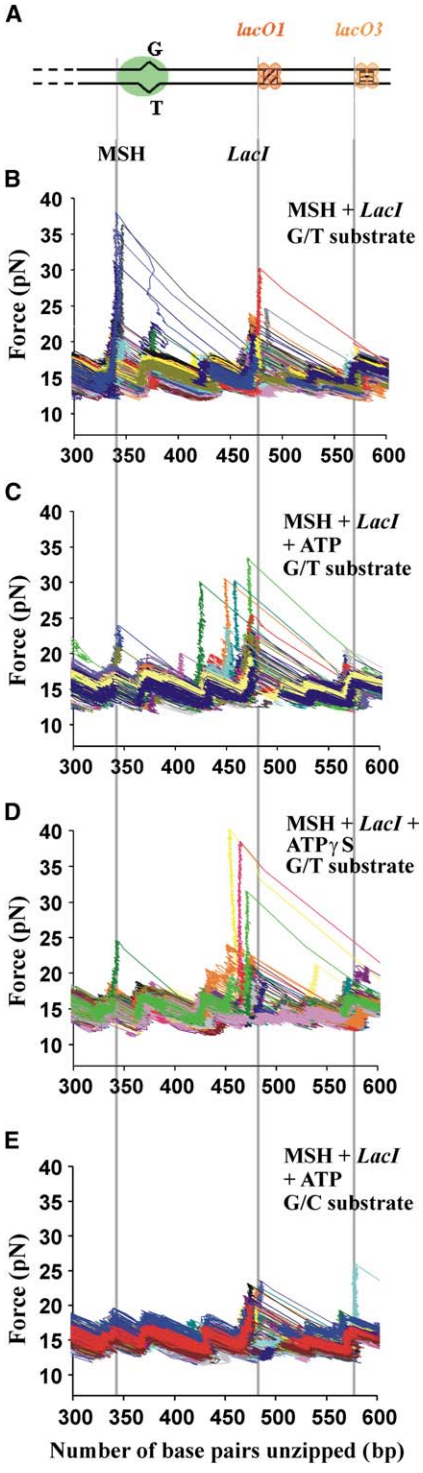


Figure 6. ATP-Induced Release of MSH2-MSH6 from the G/T Substrate Containing a LacI Blockade

(A) Cartoon showing the G/T DNA substrate bound with MSH2-MSH6 and LacI.

(B and C) Individual force traces are shown for the G/T substrate incubated in the presence of 8 nM of MSH2-MSH6 and 5 nM of LacI in the absence ([B], n = 83) or presence of 20 μM ATP ([C], n = 88). In (B), an elevated force peak consistent with LacI binding was observed at 473 ± 2 bp (SD) in addition to the MSH2-MSH6 elevated force peak (342 ± 3 bp [SD]). In (C), six out of 88 traces displayed elevated force events between the mismatch and *lac*O1.

DNA ends. Our results indicated that, in the presence of either ATP or ATPγS, a subset of MSH2-MSH6 initially bound to a mismatch site can be trapped onto DNA containing blocked ends.

Unzipping experiments performed in the presence of 5 nM LacI detected clustered elevated force events close to the *lacO1* site with >90% probability (n = 41, data not shown). The addition of ATP did not affect LacI binding position or occupancy (n = 38, data not shown). The G/T substrate also contains a weak LacI binding site (*lacO3*) located 92 bp downstream of the *lacO1* site, and a few elevated force events were observed at this site (5% occupancy; Figure 6). In the presence of 8 nM MSH2-MSH6 and 5 nM LacI, elevated force events were observed at both the mismatch (50% occupancy) and *lacO1* sites (94% occupancy), consistent with MSH2-MSH6 and LacI binding to their respective sites without interference (Figure 6B, n = 83).

In experiments containing MSH2-MSH6, LacI, and 20 μM ATP, six elevated force events were detected within 100 bp (17, 22, 22, 33, 49, and 69 bp) upstream of the LacI disruption site (Figure 6C, n = 88). A similar frequency of elevated force events in the same region (12, 15, 20, and 20 bp upstream of the LacI disruption site) was observed when 20 μM ATPγS was substituted for ATP (Figure 6C, n = 51). The frequency (7% ± 3% [SD]) of elevated force peaks for the experiments presented in Figure 6C was significantly higher than that observed in a 100 bp unblocked homoduplex DNA region (2.7% ± 0.7% [SD], p = 0.01, Figure 3A). Thus, it is unlikely that the elevated force events observed in Figure 6C were due to nonspecific binding or sticking of the DNA substrate to the sample chamber. Such events were not observed in experiments performed with LacI and MSH2-MSH6 in the absence of ATP (Figure 6B), or with LacI alone in the presence or absence of ATP (data not shown). These results suggest that these events represented ATP bound MSH2-MSH6 trapped by the LacI blockade. However, the fact that only a small percentage of MSH2-MSH6 could be trapped in this manner (~15% based on 50% initial occupancy in the absence of ATP) suggests that ATP can also induce the release of MSH2-MSH6 from a mismatch site by direct dissociation or by sliding followed by direct dissociation (Mendillo et al., 2005).

Gradia et al. (1997, 1999) proposed that the mismatch site serves as an entry point for MSH proteins to form a sliding clamp. To test this, the experiments above were repeated with a homoduplex G/C substrate containing the *lac*O1 site at the same position as with the G/T substrate. We were unable to detect MSH2-MSH6 binding to homoduplex G/C substrate in the absence (Figure 3D) or presence of ATP (Figure 6E, n = 61). These data are consistent with the elevated force events resulting from MSH2-MSH6 initially binding to the mismatch site in the G/T substrate, followed by dissociation from the site by sliding along DNA.

(D) Conditions were identical to those in (C), except 20 μM ATPγS was substituted for ATP. Elevated force events were observed upstream of *lac*O1 (four events out of 51 traces).

(E) Individual force traces (n = 61) for the homoduplex G/C substrate incubated with 8 nM MSH2-MSH6, 5 nM LacI, and 20 μM ATP.

## Discussion

We used a single-molecule unzipping assay to detect both high-affinity binding and sliding clamp modes for the *S. cerevisiae* MSH2-MSH6 MMR complex. As discussed below, this method could sensitively detect MSH2-MSH6-DNA interactions that appear important for signaling downstream steps in MMR.

### Unzipping Force Analysis Can Detect the Presence of Single Mismatches in Duplex DNA

Theoretical studies have suggested that unzipping force analysis is capable of detecting mismatches in DNA at base pair resolution. These studies, which are based on the base pair energies of the DNA duplex, predict that the unwinding force should decrease when a mismatch is encountered, and the magnitude of such a force drop is expected to depend on the binding strength of the mismatch as well as its neighboring sequence (M.D.W., unpublished data). These predictions were tested and confirmed by our study: the average unzipping force curves on templates containing a single G/T mismatch or +1 insertion showed a significant drop in unzipping force around the site of the mismatch compared to the corresponding homoduplex (Figure 2). In particular, the +1 insertion changed the local unzipping force from a peak to a dip (Figure 2B). Our results should encourage researchers to use the single-molecule unzipping assay as a tool to examine differences in unwinding force for different types of mismatches (e.g., base-base and insertion/deletion) as well as sites containing DNA adducts or other types of DNA damage in the presence and absence of DNA repair proteins.

### MSH2-MSH6 Binds to Mismatch DNA with High Specificity

It is hard to reconcile the moderate selectivity of MSH2-MSH6 for mismatch DNA (10- to 30-fold higher than homoduplex) as measured in gel shift and filter binding assays with its high selectivity in vivo, where it is estimated that MSH proteins are present at 200 (*E. coli*; Feng et al. [1996]) to 1000 (mammalian; Gradia et al. [1997]) complexes per cell. One explanation is that gel shift assays enhance binding to homoduplex DNA due to nonspecific binding and/or caging effects. In support of this, recent studies have shown that MSH proteins display a DNA end binding activity (Mendillo et al., 2005; Yang et al., 2005). We were unable to test for such an activity because we could not accurately measure unwinding force at the ends of our DNA substrates. Alternatively, it is possible that the overall specificity of the MMR reaction results from the combinatorial interactions of multiple components.

Our study indicates that the high specificity of MMR is imposed by the MSH proteins rather than a combinatorial action of multiple MMR components. We estimate that the $K_d$ for MSH2-MSH6 binding to homoduplex DNA is at least several-thousand-fold higher than for binding to mismatch sites and suggest that MSH2-MSH6 alone displays the high selectivity required to recognize DNA biosynthetic errors in vivo. This idea is supported by genetic assays in which the MSH proteins were shown to act with high specificity for DNA mismatches in reactions that do not require downstream factors in MMR (e.g., Sugawara et al. [2004]). Finally, using atomic force microscopy analysis, Wang et al. (2003) hypothesized that *E. coli* MutS interacts with homoduplex and mismatch DNA through distinct DNA binding modes. We suggest that the in vivo selectivity of MMR is due to the formation of distinct binding states by the MSH proteins on homoduplex and mismatch DNA (Wang et al., 2003) as well as to the 1000-fold difference in binding frequency of MSH proteins to these substrates (this study; Yang et al. [2005]).

### MSH2-MSH6 Shows an Asymmetric Binding Pattern on Mismatch DNA Consistent with Binding in a Specific Orientation

In vitro footprinting analysis of the yeast and human MSH2-MSH6 proteins bound to mismatch DNA indicates that both of these complexes confer an asymmetric protection pattern on DNA surrounding a mismatch site (Kijas et al., 2003; Gradia et al., 1997). We identified a similar asymmetric pattern for both the G/T and +1 mismatches by mapping the elevated force peak locations on both sides of the DNA mismatch and by comparing the magnitude of the unzipping force at each boundary. Structural analysis suggested that the MutS homodimer interacts with mismatched substrates in an asymmetric manner with respect to the mismatch site and DNA backbone contacts (reviewed in Kunkel and Erie [2005]). This is consistent with our results above indicating that MSH2-MSH6 displays orientation-specific binding to mismatch DNA.

It is not clear whether orientation-specific MSH binding is significant for MMR. Studies involving *E. coli* and human cell extracts have shown that mismatch-provoked excision in these systems is bidirectional (Grilley et al., 1993; Fang and Modrich, 1993). Does orientation-specific binding by MSH2-MSH6 confer directionality to the excision process (5′- or 3′-directed excision relative to the mismatch site)? Such an idea is supported by the finding that PCNA, a factor implicated in strand discrimination in MMR, interacts with the N-terminal tail of MSH6 (Clark et al., 2000; Flores-Rozas et al., 2000; Kleczkowska et al., 2001), and by in vitro studies suggesting that 5′- and 3′-directed excision require different subsets of MMR factors (Dzantiev et al., 2004; Zhang et al., 2005). Alternatively, binding orientation might not be relevant to the directionality of excision if downstream factors interact with the MSH proteins in an orientation-independent fashion to activate strand discrimination and excision processes.

### Direct Evidence for ATP-Dependent MSH2-MSH6 Sliding on DNA

A variety of assays have shown that ATP reduces the relative affinity of MSH proteins for mismatch and homoduplex DNA (reviewed in Kunkel and Erie [2005]). Using a real-time reversible end-blocking system, Mendillo et al. (2005) observed that MSH2-MSH6 showed ATP-dependent dissociation through DNA ends as well as by direct dissociation. Our results match nicely with those made by Mendillo et al. (2005). As shown in Figure 6, we detected elevated force events between the DNA mismatch and the LacI block upon addition of ATP for ~15%, assuming ~50% original occupancy, of the MSH2-MSH6 molecules that were initially bound to

mismatch DNA in the absence of ATP. Furthermore, the detection of elevated force events required a mismatch substrate, consistent with models in which mismatch bound MSH2-MSH6 is converted to a form that rapidly dissociates from DNA ends in the presence of ATP (Gradia et al., 1999; Mendillo et al., 2005; Blackwell et al., 1998, 2001). A drawback of our system is that it is not possible to determine whether the sliding-like signature exhibited by MSH2-MSH6 is directional or the result of random diffusion. The DNA-unzipping method is itself directional, and a high force occurs at the beginning of the unzipping procedure that might obscure elevated force signatures that occur near the unwinding start site. Assays that allow one to monitor MSH proteins on mismatch substrates are more likely to answer this question.

In the ATPγS experiment, the four elevated force events mapped 12, 15, 20, and 20 bp upstream of the LacI binding site. As shown above, MSH2-MSH6 displays an ~20 bp footprint on mismatch DNA (Figure 5). These observations, coupled with the 2–3 bp resolution limits of our mapping technique, are consistent with all four events representing a single MSH2-MSH6 molecule located immediately adjacent to bound LacI. In the presence of ATP, the six elevated force events mapped 17, 22, 22, 33, 49, and 67 bp upstream of the LacI binding site. Like the ATPγS experiment, three of the events (17, 22, and 22 bp) are consistent with a single MSH2-MSH6 molecule located adjacent to bound LacI. The other three events were located at distances from the LacI binding site that could be represented as multiples of the 16–20 bp MSH2-MSH6 footprint, with the 33 bp distance representing two sites, 49 bp representing three and 67 bp representing four. One interpretation of these data consistent with work presented by Gradia et al. (1999) is that these elevated force events represent multiple loadings of MSH2-MSH6 onto the G/T mismatch template followed by dissociation through the DNA ends. Because of the directionality of the unzipping method, we cannot determine if the observed elevated force events in the presence of ATP indicate the location of MSH2-MSH6 prior to unzipping force analysis or the displacement of the complex toward the LacI barrier by the unzipping fork.

Consistent with models proposed by both the Modrich and Fishel groups, unzipping force analysis enabled us to detect the ATP-dependent dissociation of MSH2-MSH6 from mismatch DNA through DNA ends (Blackwell et al., 1998; Gradia et al., 1999). However, unlike Mendillo et al. (2005) and models proposed by the Modrich group (Blackwell et al., 1998, 2001), we also detected this dissociation mode in the presence of ATPγS, suggesting that this type of dissociation does not require ATP hydrolysis. Our studies do not directly address aspects of a model proposed by Junop et al. (2001), in which the ATPase activity of MSH proteins acts in a proofreading role to verify mismatch recognition and authorize repair. This and other models will require analysis of early MMR steps in the presence of additional MMR components.

## Experimental Procedures

### Enzymes and Oligonucleotides

MSH2-MSH6 was purified as described by Kijas et al. (2003), and MSH2-MSH3 was purified by modifying a procedure described by Habraken et al. (1996). Oligonucleotides were purchased from IDT. Restriction enzymes, T4 DNA ligase, Klenow, and alkaline phosphatase (calf intestinal) were purchased from New England Biolabs and used as recommended. *Taq* polymerase and PfuTurbo were purchased from Fisher and Stratagene, respectively, and used in 50 μl reactions as recommended by the manufacturer. PCR reactions used to create the unzipping substrates were performed in 50 μl reaction volumes for 30 cycles with 30 s denaturation (94ºC), 30 s reannealing (52ºC), and 1.5 min (72ºC) extension steps.

### DNA Substrates

The DNA substrates used in unzipping analysis were created using methods described by Koch et al. (2002) (Figure 1). Briefly, they were constructed by ligating a 1122 bp anchoring segment containing a digoxigenin (dig) label to a 704 or 1091 bp unzipping segment containing a G/T, +1 (+G insertion), or +8 (GTGTGTGT insertion) mismatch. The unzipping segment for all of the substrates used in this study contains a biotin-dT nucleotide 13 bases from its 5′ end. The anchoring segment was created by PCR in a reaction containing *Taq* polymerase, the plasmid pRL574 (Schafer et al., 1991), and the dig-labeled forward primer (5′ dig-GTTGTA AAACGACGGCCAG TGAAT) and the *rpoB* reverse primer (5′ CCGTGATCCAGATCG TTGGT). The resulting PCR fragment was digested with BstXI prior to ligating it to an unzipping segment.

Seven different unzipping substrates, homoduplex G/C, homoduplex reverse (G/C-R), G/T, G/T reverse (G/T-R), +1, +1 reverse, (+1-R) and +8 (Figures 1–3), were constructed using an identical procedure. For this reason, only construction of the homoduplex G/C, G/T, and G/T-R (Supplemental Data) substrates will be described, and specific information on the other substrates can be obtained upon request.

The 1091 bp G/T unzipping segment contains a single G/T mismatch 356 bp downstream of the biotin label (Figure 1B). This segment was created by denaturing and then reannealing DNA fragments that were PCR amplified from pEAM128 and pEAM129 templates. These plasmids, derived from pRS425 (Christianson et al., 1992), are identical except at a single base pair position located at overlapping XhoI and HindIII restriction sites. The sequence of these plasmids is available upon request. The G/C DNA fragment (Figures 1D–1I) was generated by PCR in a reaction containing PfuTurbo, pEAM128, and primers AO1210 (5′CTGGTTTAGAGCT-BiodT-GACGGGGAAA) and AO1211 (5′ CGAACGACCTACACCGAACT). The A/T DNA fragment (Figures 1D–1I) was created by PCR in a reaction containing PfuTurbo, pEAM129, and primers AO1209 (5′CGATCTGGTTTAGAGCTTGAC GGGGAAA) and AO1211.

The G/C and A/T DNA fragments described above (2.5 μg each) were incubated at 95ºC for 7.5 min and then cooled to 24ºC over 2 hr in a 100 μl reaction containing 1 × New England Biolabs restriction enzyme Buffer 3. Four different DNA substrates (G/T, G/C, A/C, A/T; Figures 1D–1I) were expected to form as the result of the denaturation and renaturation steps. The G/T and A/C substrates can be distinguished from the G/C and A/T substrates because the single mismatches in these DNA fragments disrupt the recognition sequences of the XhoI (G/C) and HindIII (A/T) restriction enzymes. After the denaturation and reannealing steps described above, approximately 50% of the duplex DNA could not be digested by XhoI and HindIII. The reannealed products were treated with alkaline phosphatase to remove the 5′ phosphate groups. Because the AO1209 primer contains a four nucleotide 5′CGAT extension relative to primer AO1210, only the G/T mismatch substrate contains a sticky 3′ end complementary to the BstXI-digested anchoring segment. Thus, after performing a ligation reaction containing the anchoring segment and the alkaline phosphate-treated reannealed substrates, only the nicked mismatch substrate (G/T) shown in Figure 1B should be generated. To create a nicked homoduplex (G/C) substrate, pEAM128 was used as a template in two separate PCR reactions, one containing primers AO1209 and AO1211 and the other AO1210 and AO1211. The products from these reactions were mixed, denatured, and renatured and then ligated to the anchoring segment to create the homoduplex G/C substrate.

The homogeneity of the mismatch substrates created by the method outlined in Figure 1 was assessed by unzipping assay (Figure 2). For the +8 substrate, 28 out of 28 traces displayed reduced force at the predicted mismatch position (Figure 2). A control

experiment was performed to test whether the mismatch substrates were contaminated due to nonspecific ligation of the reannealing mixture to the anchoring segment (Figure 1C). This was performed by attempting to ligate the anchoring segment to the two PCR products shown in Figures 1C–1I) without performing denaturing and reannealing steps. A full-length substrate should not be created because the two PCR products lack the 3′ overhang required for ligation to the anchoring segment (Experimental Procedures). Nevertheless, substrates resulting from this ligation were tested to see if they could be tethered via a microsphere to the surface of the sample chamber (Figure 1A). These substrates yielded a tether density less than 5% of that seen for a correct substrate. When subject to unzipping, none of the tethers displayed the unzipping signature expected for a full-length DNA substrate.

### Single-Molecule Data Acquisition and Analysis

All of the single-molecule experiments were performed in 10 μl reactions at room temperature (24°C) in a sample chamber containing 0.1 pM homoduplex or mismatch unzipping substrate and 1× binding buffer (20 mM HEPES [pH 8.0], 40 μg/ml acetylated BSA [AcBSA], 2 mM $MgCl_2$, 1 mM DTT, 8% [w/v] sucrose, 50 mM NaCl). ATP (Amersham) and ATPγS (Roche) were included in the binding buffer as indicated. MSH protein was then added to the sample chamber, and the reaction was incubated at room temperature for 10 min, after which DNA molecules were analyzed by unzipping in a time interval that did not exceed 50 min in the absence of ATP and 15 min in the presence of ATP or ATPγS. We found that the binding of MSH2-MSH6 to mismatch DNA in the absence of ATP did not change significantly in this interval in an equilibrium system, and for the ATP experiments, we estimate based on the $k_{cat}$ of MSH2-MSH6 (Kijas et al., 2003) that at most 12% of input ATP was hydrolyzed at the end of the 15 min data collection period. This process was repeated to reach the indicated number of traces shown for each experiment. For the plasmid competitor study, MSH2-MSH6 was preincubated with plasmid DNA in binding buffer for 5 min prior to adding it to the sample chamber containing mismatch substrate in 1× binding buffer. The reaction was further incubated for 10 min, after which unzipping was performed as above.

The configuration of the unzipping assay shown in Figure 1A is the same as described previously (Koch et al., 2002). Dig-labeled DNA substrates (homoduplex or mismatch) were anchored to glass coverslips coated with anti-dig antibody (Fisher). Streptavidin-coated 0.48 μm diameter microspheres were then incubated with the dig-anchored substrates to attach a single microsphere to a biotin-labeled nucleotide located near the 5′ side of the nick. The microsphere was then trapped by a focused 1064 nm laser beam, and the duplex DNA was unwound from the nick site under conditions in which the coverslip was moved away from the optical trap at a constant velocity (30 nm/s). During unwinding, the intensity of the laser was under feedback control in order to maintain the microsphere at constant distance from the trap center.

The relationships between the unzipping force versus the number of base pairs unzipped shown in this study were determined from the force calibration data and the double- and single-strand DNA elasticity parameters (Wang et al., 1997; Koch et al., 2002). Because A/T and G/C base pairs display different base pairing energies, the naked DNA-unzipping force is sequence dependent, and its pattern is highly reproducible (Bockelmann et al., 1997, 1998; Essevaz-Roulet et al., 1997). Thus, by using the energy values of 4.37 $k_BT$ and 1.33 $k_BT$ for G/C and A/T bonds, respectively, where $k_BT$ indicates thermal energy, the force versus number of base pairs unzipped relation can be predicted. The patterns of the theoretical and experimental curves agree well with each other but are shifted relative to each other in the number of base pairs unzipped axis due to uncertainties in measuring the DNA end-to-end distance. To obtain a more accurate number of base pairs unzipped values, the experimental and theoretical curves were crosscorrelated. The offset of the correlation peak from zero displacement represents the amount of relative shift between the two curves. The experimental curve was then shifted by this amount to align with the theoretical curve. This alignment step allows us to determine the number of base pairs unzipped to near base pair accuracy.

Control experiments were performed to confirm that the crosscorrelation method could be used to accurately align different DNA templates. We constructed an unzipping template containing both G/T and T/G (reverse G/T) mismatches on the same DNA template separated by 107 bp. Because mismatch binding is subject to sequence context (e.g., Marsischky and Kolodner [1999]), the mismatches were created using the same nine base pair sequence surrounding both mismatch sites. The unzipping patterns obtained with this double-mismatch substrate in the presence of 8 nM MSH2-MSH6 did not show any detectable difference in binding position for the two sites relative to DNA substrates that contained only one of the two sites (data not shown). This control indicated that the forward and reverse G/T and +1 substrates described in Figure 5 could be aligned with respect to binding position with high accuracy. An extensive description of the crosscorrelation method will be presented elsewhere (M. Hall, A. Shundrovsky, and M.D.W., unpublished data).

### Identification of Elevated Force Peaks

Elevated force events were identified by analyzing the unzipping force along a DNA template in the presence and absence of MSH2-MSH6 or *lac* repressor (LacI). To analyze the cluster of elevated force events that were observed in the presence of protein in the vicinity of the protein binding site, we focused on a 30 bp window that contained these peaks and collected unzipping force measurements for each trace within the window. The window size was chosen so that it was large enough to accommodate all the peaks in the cluster but small enough to avoid background noise. In practice, varying the window size from 15 to 50 bp did not affect the analysis. In the presence of protein, the histogram displayed a bimodal distribution that was fit to a double Gaussian function. The Gaussian centered at the lower force levels, which aligns well with that of naked DNA, represents the population without protein binding. By setting the intersection point of the two Gaussian functions as a threshold, traces with a higher peak force were designated as those involving protein binding. For all the data points located in an identified elevated force peak, the corresponding template positions were averaged to obtain the final peak position.

### Statistical Analysis

For $N$ sites probed and $M$ binding events identified, the standard deviation of the uncertainty, as measured by the occupation ratio, $\sigma$ = M/N, was determined by $\sqrt{\sigma(1-\sigma)}/\sqrt{N}$. The Student's t test (http://faculty.vassar.edu/lowry/VassarStats.html) was used to determine whether the difference between the mean of two data sets was statistically significant. For example, to compare the unzipping force on the G/T and the G/C homoduplex templates, the force at bp 356 (G/T in the G/T substrate, G/C in the homoduplex substrate) in each individual trace was measured and subject to the Student's t test. P values less than 0.05 indicated that the difference between the two data sets was significant.

### Supplemental Data

Supplemental Data include text and one figure and can be found with this article online at http://www.molecule.org/cgi/content/full/20/5/771/DC1/.

### Acknowledgments

We thank Alla Shundrovsky, Jianyong Tang, and Micheal Mwangi for technical advice; Tatiana Velikodvorskaya and Robert Weissberg for providing *lac* repressor; and Eric Greene, John Lis, and Jeff Roberts for helpful comments and technical advice. J.J. and E.A. were supported by NIH research grant GM53085 and Z.G. by a Cornell Presidential Research Scholars Fellowship. J.A.S. is a Research Fellow of the National Cancer Institute of Canada supported with funds provided by the Terry Fox Run. M.D.W. was supported by NIH research grant GM59849 and the Keck Foundation's Distinguished Young Scholar Award.

Received: August 19, 2005
Revised: September 28, 2005
Accepted: October 11, 2005
Published: December 8, 2005

## References

Allen, D.J., Makhov, A., Grilley, M., Taylor, J., Thresher, P., Modrich, P., and Griffith, J.D. (1997). MutS mediates heteroduplex loop formation by a translocation mechanism. EMBO J. *16*, 4467–4476.

Blackwell, L.J., Martik, D., Bjornson, K.P., Bjornson, E.S., and Modrich, P. (1998). Nucleotide-promoted release of hMutSα from heteroduplex DNA is consistent with an ATP-dependent translocation mechanism. J. Biol. Chem. *273*, 32055–32062.

Blackwell, L.J., Bjornson, K.P., Allen, D.J., and Modrich, P. (2001). Distinct MutS DNA-binding modes that are differentially modulated by ATP binding and hydrolysis. J. Biol. Chem. *276*, 34339–34347.

Bockelmann, U., Essevaz-Roulet, B., and Heslot, F. (1997). Molecular stick-slip motion revealed by opening DNA with piconewton forces. Phys. Rev. Lett. *79*, 4489–4492.

Bockelmann, U., Essevaz-Roulet, B., and Heslot, F. (1998). DNA strand separation studied by single molecule force measurements. Phys. Rev. E *58*, 2386–2394.

Bowers, J., Tran, P.T., Liskay, R.M., and Alani, E. (2000). Analysis of yeast MSH2–MSH6 suggests that the initiation of mismatch repair can be separated into discrete steps. J. Mol. Biol. *302*, 327–338.

Christianson, T.W., Sikorski, R.S., Dante, M., Shero, J.H., and Hieter, P. (1992). Multifunctional yeast high-copy-number shuttle vectors. Gene *110*, 119–122.

Clark, A.B., Valle, F., Drotschmann, K., Gary, R.K., and Kunkel, T.A. (2000). Functional interaction of proliferating cell nuclear antigen with MSH2-MSH6 and MSH2-MSH3 complexes. J. Biol. Chem. *275*, 36498–36501.

Dzantiev, L., Constantin, N., Genschel, J., Iyer, R.R., Burgers, P.M., and Modrich, P. (2004). A defined human system that supports bidirectional mismatch-provoked excision. Mol. Cell *15*, 31–41.

Essevaz-Roulet, B., Bockelmann, U., and Heslot, F. (1997). Mechanical separation of the complementary strands of DNA. Proc. Natl. Acad. Sci. USA *94*, 11935–11940.

Evans, E. (2001). Probing the relation between force—lifetime—and chemistry in single molecular bonds. Annu. Rev. Biophys. Biomol. Struct. *30*, 105–128.

Fang, W.H., and Modrich, P. (1993). Human strand-specific mismatch repair occurs by a bidirectional mechanism similar to that of the bacterial reaction. J. Biol. Chem. *268*, 11838–11844.

Feng, G., Tsui, H.C., and Winkler, M.E. (1996). Depletion of the cellular amounts of the MutS and MutH methyl-directed mismatch repair proteins in stationary-phase *Escherichia coli* K-12 cells. J. Bacteriol. *178*, 2388–2396.

Flores-Rozas, H., Clark, D., and Kolodner, R.D. (2000). Proliferating cell nuclear antigen and Msh2p-Msh6p interact to form an active mispair recognition complex. Nat. Genet. *26*, 375–378.

Gradia, S., Acharya, S., and Fishel, R. (1997). The human mismatch recognition complex hMSH2-hMSH6 functions as a novel molecular switch. Cell *91*, 995–1005.

Gradia, S., Subramanian, D., Wilson, T., Acharya, S., Makhov, A., Griffith, J., and Fishel, R. (1999). hMSH2-hMSH6 forms a hydrolysis-independent sliding clamp on mismatched DNA. Mol. Cell *3*, 255–261.

Grilley, M., Griffith, J., and Modrich, P. (1993). Bidirectional excision in methyl-directed mismatch repair. J. Biol. Chem. *268*, 11830–11837.

Habraken, Y., Sung, P., Prakash, L., and Prakash, S. (1996). Binding of insertion/deletion DNA mismatches by the heterodimer of yeast mismatch repair proteins MSH2 and MSH3. Curr. Biol. *6*, 1185–1187.

Heinen, C.D., Schmutte, C., and Fishel, R. (2002). DNA repair and tumorigenesis: lessons from hereditary cancer syndromes. Cancer Biol. Ther. *1*, 477–485.

Hess, M.T., Gupta, R.D., and Kolodner, R.D. (2002). Dominant *Saccharomyces cerevisiae msh6* mutations cause increased mispair binding and decreased dissociation from mispairs by Msh2-Msh6 in the presence of ATP. J. Biol. Chem. *277*, 25545–25553.

Iaccarino, I., Marra, G., Palombo, F., and Jiricny, J. (1998). hMSH2 and hMSH6 play distinct roles in mismatch binding and contribute differently to the ATPase activity of hMutSα. EMBO J. *17*, 2677–2686.

Joshi, A., Sen, S., and Rao, B.J. (2000). ATP-hydrolysis-dependent conformational switch modulates the stability of MutS-mismatch complexes. Nucleic Acids Res. *28*, 853–861.

Junop, M.S., Obmolova, G., Rausch, K., Hsieh, P., and Yang, W. (2001). Composite active site of an ABC ATPase: MutS uses ATP to verify mismatch recognition and authorize DNA repair. Mol. Cell *7*, 1–12.

Kijas, A.W., Studamire, B., and Alani, E. (2003). *msh2* separation of function mutations confer defects in the initiation steps of mismatch repair. J. Mol. Biol. *331*, 123–138.

King, R.A., Sen, R., and Weisberg, R.A. (2003). Using a *lac* repressor roadblock to analyze the *E. coli* transcription elongation complex. Methods Enzymol. *371*, 207–218.

Kleczkowska, H.E., Marra, G., Lettieri, T., and Jiricny, J. (2001). hMSH3 and hMSH6 interact with PCNA and colocalize with it to replication foci. Genes Dev. *15*, 724–736.

Koch, S.J., Shundrovsky, A., Jantzen, B.C., and Wang, M.D. (2002). Probing protein-DNA interactions by unzipping a single DNA double helix. Biophys. J. *83*, 1098–1105.

Kunkel, T.A., and Erie, D.A. (2005). DNA mismatch repair. Annu. Rev. Biochem. *74*, 681–710.

Marsischky, G.T., and Kolodner, R.D. (1999). Biochemical characterization of the interaction between the *Saccharomyces cerevisiae* MSH2-MSH6 complex and mispaired bases in DNA. J. Biol. Chem. *274*, 26668–26682.

Mendillo, M.L., Mazur, D.J., and Kolodner, R.D. (2005). Analysis of the interaction between the *Saccharomyces cerevisiae* MSH2-MSH6 and MLH1-PMS1 complexes with DNA using a reversible DNA end-blocking system. J. Biol. Chem. *280*, 22245–22257.

Schafer, D.A., Gelles, J., Sheetz, M.P., and Landick, R. (1991). Transcription by single molecules of RNA polymerase observed by light microscopy. Nature *352*, 444–448.

Schofield, M.J., and Hsieh, P. (2003). DNA mismatch repair: molecular mechanisms and biological function. Annu. Rev. Microbiol. *57*, 579–608.

Schofield, M.J., Nayak, S., Scott, T.H., Du, C., and Hsieh, P. (2001). Interaction of *Escherichia coli* MutS and MutL at a DNA mismatch. J. Biol. Chem. *276*, 28291–28299.

Sia, E.A., Kokoska, R.J., Dominska, M., Greenwell, P., and Petes, T.D. (1997). Microsatellite instability in yeast: dependence on repeat unit size and DNA mismatch repair genes. Mol. Cell. Biol. *17*, 2851–2858.

Sugawara, N., Goldfarb, T., Studamire, B., Alani, E., and Haber, J.E. (2004). Heteroduplex rejection during single-strand annealing requires Sgs1 helicase and mismatch repair proteins Msh2 and Msh6 but not Pms1. Proc. Natl. Acad. Sci. USA *101*, 9315–9320.

Wang, M.D., Yin, H., Landick, R., Gelles, J., and Block, S.M. (1997). Stretching DNA with optical tweezers. Biophys. J. *72*, 1335–1346.

Wang, H., Yang, Y., Schofield, M.J., Du, C., Fridman, Y., Lee, S.D., Larson, E.D., Drummond, J.T., Alani, E., Hsieh, P., and Erie, D.A. (2003). DNA bending and unbending by MutS govern mismatch recognition and specificity. Proc. Natl. Acad. Sci. USA *100*, 14822–14827.

Yang, Y., Sass, L.E., Du, C., Hsieh, P., and Erie, D.A. (2005). Determination of protein-DNA binding constants and specificities from statistical analyses of single molecules: MutS-DNA interactions. Nucleic Acids Res. *33*, 4322–4334.

Zhang, Y., Yuan, F., Presnell, S.R., Tian, K., Gao, Y., Tomkinson, A.E., Gu, L., and Li, G.-M. (2005). Reconstitution of 5′ directed human mismatch repair in a purified system. Cell *122*, 693–705.